Luminescence of CsI:Na crystal scintillator under synchrotron radiation excitation

*K. Shunkeyev[1], A. Kenzhebayeva[1], Sh. Sagimbayeva[1], Y. Syrotych[2], *Yu. Zorenko[1,2,3]

[1]*K. Zhubanov Aktobe Regional University, 34 A. Moldagulova Ave., 030000 Aktobe, Kazakhstan*
[2]*Department of Physics, Kazmierz Wielki University in Bydgoszcz, Powstańców Wielkopolskich str., 2, 85-0906 Bydgoszcz, Poland*
[3]*Medical Physics Department, Prof. Franciszek Łukaszyk Oncology Center, I. Romanowska str., 2, 85-796 Bydgoszcz, Poland*
**e-mail of the corresponding authors: kuanyshbek.sh.01@gmail.com, zorenko@ukw.edu.pl*

Abstract: This work investigates the luminescence properties and energetic structure of emission centers created by Na_{Cs} isoelectronic impurities in a well-known CsI:Na scintillation crystal. Using synchrotron radiation excitation at 8 K, high-resolution spectroscopic techniques were employed to probe the electronic transitions and luminescent dynamics within the crystal. The study reveals distinct emission bands that can be attributed to both self-trapped exciton (STE) states and excitons bound to Na_{Cs} and defect-related centers, with a clear separation between fast and slow decay components. These findings provide deeper insight into how the Na_{Cs} impurity alters the emission behaviour of the CsI host, including modifications to energy transfer and relaxation processes.

Keywords: scintillators, CsI, Na impurity, luminescence, synchrotron radiation

1. Introduction

Sodium-doped cesium iodide (CsI:Na) crystals represent a good alternative to NaI:Tl and CsI:Tl scintillation crystals in various applications. This is due to their high radioluminescence (RL) light yield (approximately 85% that of NaI:Tl), a broad emission band covering the 300–600 nm spectral region with a maximum in the blue (420 nm) where the most popular photomultiplier tubes (PMTs) with bialkali S20 photocathodes exhibit peak sensitivity, and significantly lower hygroscopicity compared to NaI:Tl [1–3]. In addition, the CsI host has a relatively high density (4.5 g/cm³) and an effective atomic number of $Z_{eff} = 54$, along with excellent mechanical strength and thermal stability. As a result, CsI:Na crystals are extensively used in geophysical and cosmic space equipment [1–3]. They are also employed in non-destructive testing (defectoscopy) and in experimental high-energy physics as scintillation elements in electromagnetic calorimeters [3]. The light yield of CsI:Na scintillators reaches its maximum at about –80 °C, making the material suitable for scintillation applications at both low and high temperatures [3]. Furthermore, the average scintillation decay time of CsI:Na crystals at room temperature is approximately 630 ns, which is shorter than that of CsI:Tl (around 1000 ns).

A drawback of both CsI:Na and CsI:Tl scintillators is their relatively high afterglow, which substantially limits the counting rate in the conventional 1000 ns time interval [3]. To overcome this limitation, it is essential to examine in detail the basic luminescent properties of the Na^+ dopant in the CsI host and its interaction with intrinsic defects of the matrix. It should be noted, however, that the properties

of CsI:Na crystals depend significantly on the material preparation conditions, dopant content, and the temperature at which measurements are made [4, 5].

For practical applications, the luminescent and scintillation properties of CsI:Na crystals have been extensively investigated using both conventional [4–6] and advanced spectroscopic methods [7–13]. However, a common limitation of many previous studies [4–6] is the lack of a clear analysis of Na^+ ions in the CsI host as *cation isoelectronic impurities* (CII) in ionic crystals, and the associated peculiarities in the luminescent properties of CsI:Na [14, 15].

Generally, A dopant acting as a CII relative to a core cation B with the same charge state, for example, Na^+ ions substituting Cs cations in the CsI matrix [14] or Sc^{3+} and Ga^{3+} ions occupying Al^{3+} sites in an Al_2O_3 host [16, 17], can effectively localize low-energy excitations (electrons, holes, or excitons) by creating a non-Coulombic potential at the substitution site [14, 15]. For this reason, CIIs are widely exploited in the development of luminescence and scintillation materials that operate in the UV and blue regions and offer good temperature stability at room temperature. Examples include alkali-halide crystals AB (where A = K, Na, or Cs; B = I, Cl, or Br) [4–6, 19] and Al_2O_3–Y_2O_3–Lu_2O_3 oxides of various structural types (such as sapphire, garnets, and perovskites) [21–26]. Among the most well-known scintillators based on these systems, which exhibit high RL light yields (up to 30–85% that of NaI:Tl), are single crystals of CsI:Na [1–3] and CsI:Li [18, 19], Al_2O_3:Sc sapphire [12], and $Y_3Al_5O_{12}$:Sc and $Lu_3Al_5O_{12}$:Sc garnets (YAG:Sc and LuAG:Sc) [21, 22].

Despite these advances, studying the luminescent properties and the electronic structure of CIIs in dielectric matrices remains challenging because these dopants typically do not possess internal transitions in the UV and visible regions that are detectable by conventional absorption or luminescence spectroscopy. A promising solution is provided by luminescence spectroscopy in the vacuum ultraviolet (VUV) range under excitation by synchrotron radiation (SR). This approach has proven effective in our work and that of other researchers investigating Sc^{3+} and Ga^{3+} CIIs in Al_2O_3 sapphire [15, 16], Sc^{3+} and La^{3+} CIIs in crystals and single-crystalline films of YAG and LuAG garnets [20, 21] as well as in YAP perovskite [22], and in studies of antisite defects (where A cations occupy the positions of B cations) that serve as analogues to CIIs in garnets and perovskites [22–25]. However, according to the available literature, VUV spectroscopy of Na^+ CII luminescence in a CsI host has not yet been performed. This gap in the research is the focus of the present work. As supporting information, our research also incorporates detailed investigations of the luminescent properties of undoped CsI under SR excitation [8–13].

2. Samples and Experimental Technique

The sample used for investigation, with dimensions of 2 × 4 × 1 mm, was prepared from a high-quality CsI:Na crystal grown by the Bridgman method in a quartz ampoule pumped out air atmosphere [3]. The Na dopant concentration in the charge for crystal growth was 0.3 at.%. The light yield (LY) of this CsI:Na crystal was approximately 40,000 photons/MeV when excited by γ-rays from a ^{137}Cs source.

Time-resolved luminescence investigations of the CsI:Na crystal were performed within the framework

of the I-20240974 EC project at the Superlumi experimental station at DESY. The measurements were carried out at 8 K under excitation by pulsed synchrotron radiation (SR) with a pulse duration of 126 ps and energies ranging from 3.7 to 25 eV. The emission and excitation spectra were recorded both in a time-integrated regime (within the limits of the SR pulse, which has a repetition period of 192 ns and a pulse duration of 126 ps) and in specific time intervals: 1.2–40 ns (fast components) and 120–192 ns (slow components) [12].

The photoluminescence (PL) emission spectra were recorded using a monochromator-spectrograph (Spectra-Pro-308i, Acton Research Corporation) equipped with a liquid nitrogen–cooled CCD camera (Princeton Instrument Inc.). When using a 300 lines/mm grating, the spectral resolution in the CsI exciton range was approximately 0.5 nm (0.025 eV). The PL emission spectra were also corrected for the CCD sensitivity.

Photoluminescence excitation (PLE) spectra were recorded with a primary monochromator resolution of approximately 0.3 nm using a Hamamatsu R6358P photomultiplier as the detector. The excitation spectra were corrected for the spectral dependence of the transmittance of the Al grating and the intensity of the SR beam. The PLE and reflection signals were accumulated over a 200-ns period defined by the SR excitation pulse repetition. The luminescence of sodium salicylate ($C_7H_5NaO_3$), with a maximum at 420 nm, is known to exhibit a constant quantum yield when excited in the 3.7–24 eV range. Therefore, the PLE spectrum measured for the 420-nm emission of sodium salicylate has been used to correct the reflectance and luminescence excitation spectra for the incident photon flux.

The reflectance spectra were registered simultaneously with PLE in one measurements circle. For the reflectance spectra measurements, the photons reflected from the sample were recorded at an angle of 35° relative to the incident beam (with an incidence angle of 17.5°). The reflection output window was coated with a thin layer of sodium salicylate to convert the reflected light into photons in the 400–440 nm range, making it suitable for detection by a Valvo XP2230 B photomultiplier tube installed on the backside. A time-resolved spectroscopy technique was used to discriminate the emission of sodium salicylate (which has a characteristic decay time constant of approximately 10 ns) from the fast component of scattered light (<1 ns).

The PL decay kinetics were recorded within a 200-ns time window between SR excitation pulses, and the PL decay curves were measured over a time range of 1.2–193 ns.

3. PL Emission Spectra of CsI:Na Crystal

The PL emission spectra of a CsI:Na crystal at 8 K under excitation by synchrotron radiation (SR) at different energies are presented in Fig. 1, both in linear scale (a) and logarithmic scale (b), to better reveal the details of these spectra. The excitation wavelengths (energies) selected correspond to the characteristic points of the PL excitation bands shown in Fig. 2.

In general, under excitation with an energy of 5.63 eV (220 nm) in the exciton range of the CsI host, the emission spectrum consists of a superposition of luminescence from Na_{Cs} centers. It is dominated by a

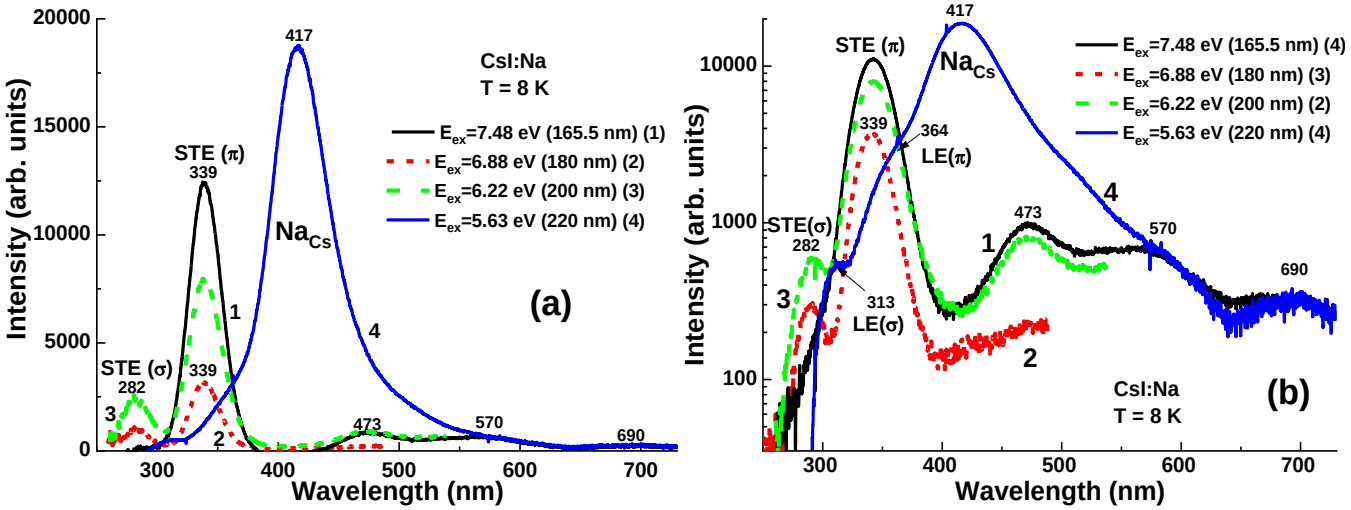

Fig.1 PL mission spectra of CsI:Na crystal at 8 K under synchrotron radiation excitation with different wavelength in the linear (a) and logarithmic (b) scale.

band peaked at 417 nm, which is attributed to the emission from excitons bound to Na_{Cs} centers (BSE), and features two bumps peaked at 313 nm and 364 nm that most likely correspond to the luminescence of localized excitons around Na_{Cs} centers (LE). It should be noted that in pure CsI crystals, with similar photoexcitation, the band peaked at 417 nm (2.95 eV) is absent from the emission spectra, which indicates its impurity nature Na_{Cs} centers.

Furthermore, when the CsI:Na crystal is excited in the 165–200 nm range (i.e., with higher energy), the well-known self-trapped exciton (STE) luminescence is observed. This luminescence exhibits bands peaking at 282 nm (σ-components) and 339 nm (π-components), corresponding to radiative transitions from the singlet and triplet excited states of the STE, respectively. According to [12], two types of STE exist in the CsI host: the *on-center* STE, which consists of an electron paired with a V_K center (i.e., a hole trapped by a halogen dimer), and the *off-center* STE, which is composed of nearest-neighbour pairs of F-centers (electrons trapped at halogen vacancies) and H-centers (interstitial halogen atoms). The excited states of both types of STE exist in thermal equilibrium in singlet and triplet configurations [12]. The emission band at 340 nm is assigned to the *off-center* STE, whereas the emission band at a shorter wavelength (290 nm) is attributed to the *on-center* STE [11, 12].

Under excitation by SR in the 165–200 nm range, additional low-intensity luminescence bands at 473 nm, 570 nm, and 690 nm are observed. These bands strongly overlap with the intense luminescence band of the Na_{Cs} centers and most likely correspond to the luminescence of localized excitons (LE) and bound state excitons (BSE) associated with several defect centers. Specifically, according to [11], these bands can be attributed to (i) the emission of excitons localized at aggregates of vacancies (λ_{max} = 470 nm) and (ii) the emission of excitons localized at non-vacancy defects (λ_{max} = 570 and 690 nm). However, because the intensity of the latter two red-range bands is very low, detailed measurements with SR for a comprehensive investigation of their nature are not feasible.

4. PL Excitation and Reflection Spectra of Different Centers in CsI:Na Crystal

4.1 PL Excitation and Reflection Spectra of STE Centers

The PLE and reflection spectra (displayed on a logarithmic scale) in the 4–25 eV range (a and b) and in greater detail in the 4.7–7 eV range (c) for the STE luminescence in the σ (a and b) and π (c and d) bands, recorded at 280 nm (a and b) and 340 nm (c and d), respectively, in a CsI:Na crystal at 8 K, are presented in Fig. 2. The positions of the maxima for all registered PLE and reflection bands are given in Table 1.

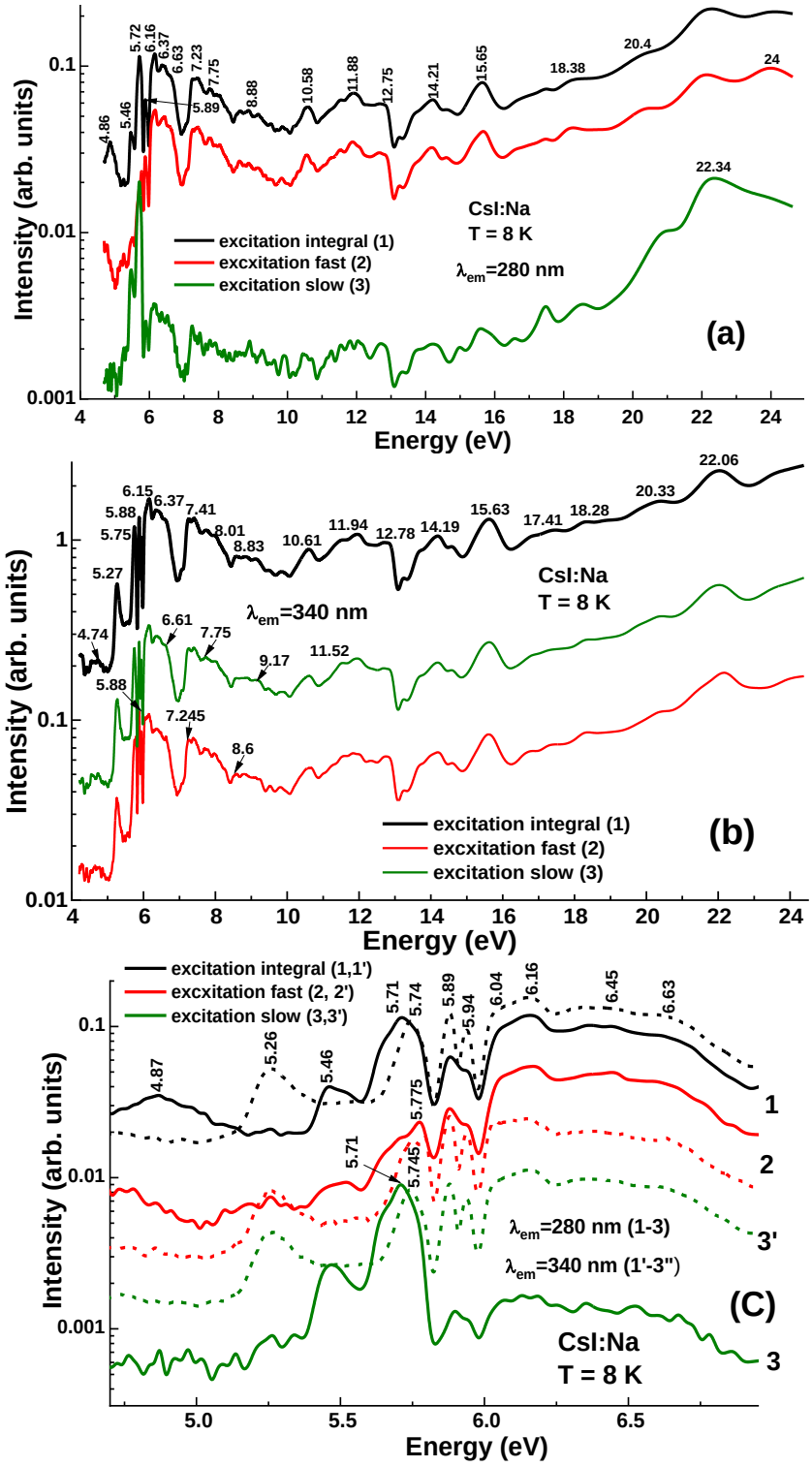

Fig.2. PLE spectra (a, c) (in the logarithmic scale) of STE emission in σ (a, c) and π (b) bands, registered at 280 nm (a, c) and 340 nm (b, c), respectively, in the CsI:Na crystal at 8 K.

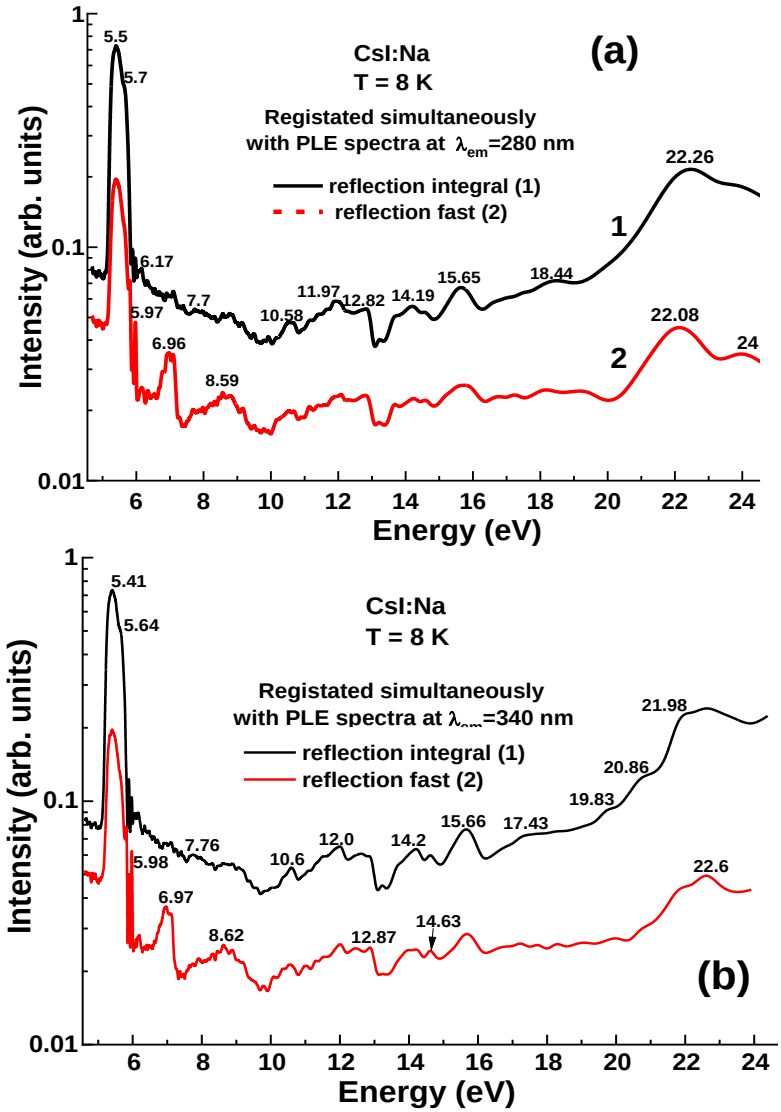

Fig.3. Reflection spectra (in the logarithmic scale), registered simultaneously with PLE spectra of luminescence at 280 nm (a) and 340 nm (b), corresponding to the STE emission in σ (a) and π (b) bands in the CsI:Na crystal at 8 K.

Table 1. Positions of PLE and reflection bands (in integral spectra) of different types of luminescence centers in CsI:Na crystals (most intensive bands are indicated by **bolt**)

Type of emission bands and their positions	**Positions of the excitation (Ex.) and reflection (Ref.) bands, eV**
STE (σ) – 280 nm	**Ex.:** *I group* (4.86, 5.46, **5.72, 6.16,** ***6.37, 6.63***); *II group* (7.23, 7.75, 8.88); *III group* (10.58, 11.88, 12.75); *IV group* (14.21, 15.65, 18.38, 20.4, 22.34, 24.0) **Ref.:** *I group* (**5.5**, **5.7**, 5.97, 6.17, 6.96); *II group* (7.7, 8.59); *III group* (10.58, 11.97, 12.83); *IV group* (14.19, 15.65, 18.44, 22.08, 22.26, 24.0)
STE (π) – 340 nm	**Ex.** : *I group* (4.74, 5.27, 5.75, **5.88, 6.15,** ***6.37, 6.61***); *II group* (7.41, 8.01, 8.83); *III group* (10.61, 11.94, 12.78); *IV group* (14.19, 15.63, 17.41, 18.28, 20.33, 22.06) **Ref.:** *I group* (**5.41**, **5.64,** 5.96, 6.17, 6.96); *II group* (7.76, 8.62); *III group* (10.6, 12.0, 12.87); *IV group* (14.2, 14.63, 15.66, 17.43, 19.83, 20.86, 22.08, 22.26, 24.0)
BSE (Na_{Cs}) – 417 nm	**Ex.**: *I group* (4.69, **5.42**, **5.69**, 5.885, 6.04); *II group* (7.27, 7.41); *III group* (10.44) **Ref.:** *I group* (4.68, 5.41, 5.66, 5.885, 5.97); *II group* (6.95, 7.13, 8.54, 8.8, 9.65)
Defect centers – 490 nm	**Ex.**: *I group* (4.27; 4.49, 4.66, 4.81; 5.04, **5.32**, **5.63**, 5.88, 5.94, 6.14, 6.31, 6.61); *II group* (7.2, 7.44, 7.75, 8.0, 8.92, 9.29)

There is a physical rationale for grouping all the PLE and reflection bands into four main categories corresponding to the specific shapes of these spectra in the following energy ranges: 4.2–7 eV, 7–10 eV, 10–13 eV, and 13–24 eV (see Fig. 2 and Table 1). In general, the principal features of the PLE reflectance spectra of the CsI:Na crystal are observed in the first range. The energy positions in the remaining three ranges appear to correspond to multiples and/or sums of the energy excitations from the first range (Ei(I)); for example, $2E_i(I)$, $3E_i(I)$, and $4E_i(I)$ or $\Sigma E_i(I)$, $\Sigma[E_i(I) + E_i(II)]$, and $\Sigma[E_i(I) + E_i(II) + E_i(III)]$ for the energy ranges II, III, and IV, respectively.

Another notable feature of the PLE spectra of STE in the σ and π emission bands is the sharp character of the PLE bands in the 5.7–6.0 eV range, most likely due to the formation of free Vanier-Mott excitons. For instance, in the PLE spectra corresponding to the σ- emission bands at 282 nm (Fig. 2a, curve 2), the intensity of the fast components is significantly higher than that of the slow components (curve 3), whereas for the π emission band at 340 nm (Fig. 2b), the intensity of the slow components (curve 3) is much higher than that of the fast ones (curve 2). The integrated PLE spectra for the σ- and π- emission bands also show slightly different positions for their main bands, peaking at 5.74 eV and 5.72 eV, respectively (Fig. 2c). Furthermore, the main maxima of the PLE spectra for the fast and slow emission components of the σ and π bands occur at different energies — 5.71 eV and 5.775 eV (Fig. 3c, curves 2 and 3) for the σ band, and 5.75 eV and 5.87 eV (Fig. 3c, curves 2 and 3) for the π band. Therefore, the energy structure of the STE in the CsI host can be described as having a singlet state at 5.72 eV, which is responsible for fast singlet–singlet radiative transitions (σ emission bands peaking at 280 nm), and a triplet state at 6.15 eV, which gives rise to slow triplet–singlet radiative transitions (π emission bands peaking at 340 nm).

This interpretation is further supported by the reflection spectra of the CsI:Na crystal, recorded at 280 nm and 340 nm (Fig. 3a and 3b, respectively). The main reflection peaks in the exciton range, observed at 5.5 and 5.7 eV, and at 5.41 and 5.64 eV, correspond to two distinct configurations (*on-site* and *off-site*) of the STE in CsI. Interestingly, the positions of these reflection bands are shifted to lower energies by approximately 0.22–0.46 eV and 0.31–0.5 eV, respectively, compared to the corresponding bands in the PLE spectra for the 280 nm and 340 nm emissions (i.e., 5.72 and 6.16 eV, and 5.88 and 6.15 eV, respectively; see Table 1). Considering that the main excitonic peaks in dielectrics are typically located about 0.9 eV below the band gap of the material [24, 26–30], the band gap of CsI can be estimated to be in the range of 6.4–6.6 eV at 8 K. Most likely, the PLE peaks at 6.37 eV and 6.63 eV (Table 1) correspond to the direct and indirect transitions in the CsI host.

4.2 PL Excitation and Reflection Spectra of Na_{Cs} and Defect-Related Emitting Centers

The PLE and reflection spectra (all on a logarithmic scale) in the 4–11 eV range for the BSE (Na_{Cs}) centers, recorded at 420 nm in the CsI:Na crystal at 8 K, are shown in Fig. 4. The positions of the maxima for all registered PLE and reflection bands are presented in Table 1.

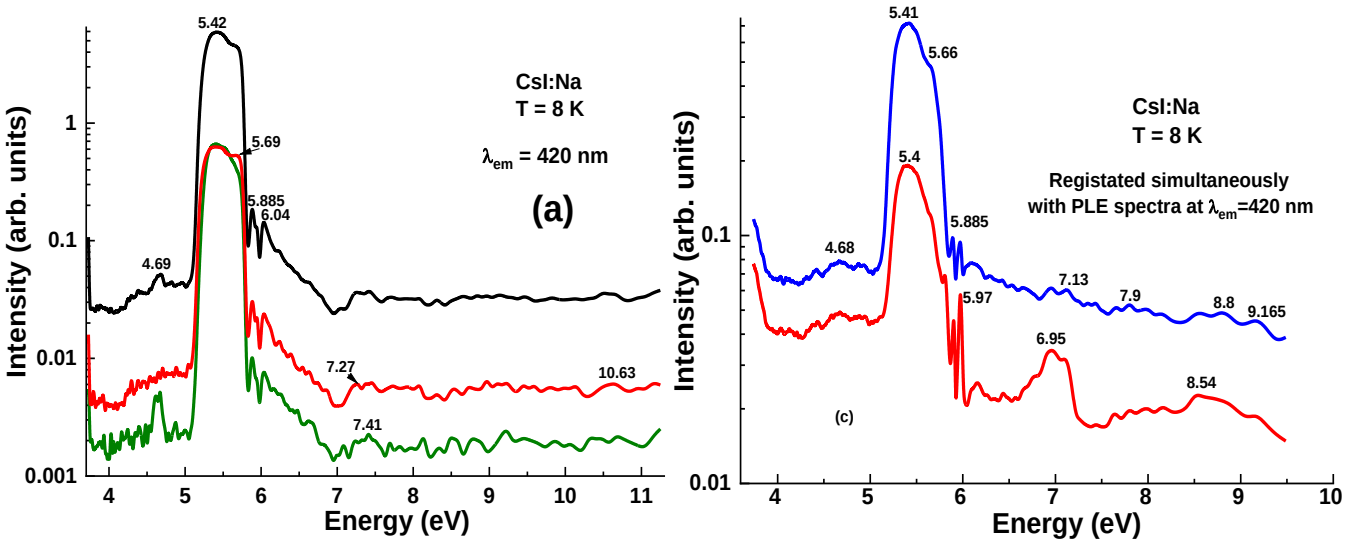

Fig.4. PLE spectra (a) and reflection (b) spectra (in the logarithmic scale) of an excitons bound with Na_{Cs} IIs (BSE(Na_{Cs} center) in the CsI:Na crystal at 8 K.

The shape of the PLE spectra for the BSE (Na_{Cs}) centers recorded at 420 nm (Fig. 4) is completely different from that of the STE spectra in CsI host (Figs. 2 and 3). Specifically, the strong PLE bands peaked at 5.42 and 5.69 eV dominate the spectra of the fast and slow emission components of these centers (Fig. 4a). Most likely, these PLE peaks correspond to the singlet–singlet and triplet–singlet transitions of excitons bound to Na_{Cs} isoelectronic impurities. The reflection spectra (Fig. 4b) also show two dominant bands, peaked at 5.41 eV (fast component) and 5.66 eV (slow component), which are only slightly shifted relative to the corresponding PLE bands (Fig. 4a). Therefore, the exciton formation energy for excitons bound to Na in the CsI host is approximately 5.41–5.42 eV.

The PLE spectrum of the emission from defect-related centers, recorded at 470 nm, associated with aggregate vacancies in the CsI:Na crystal in the band peaked at 473 nm at 8 K is shown in Fig. 5. In

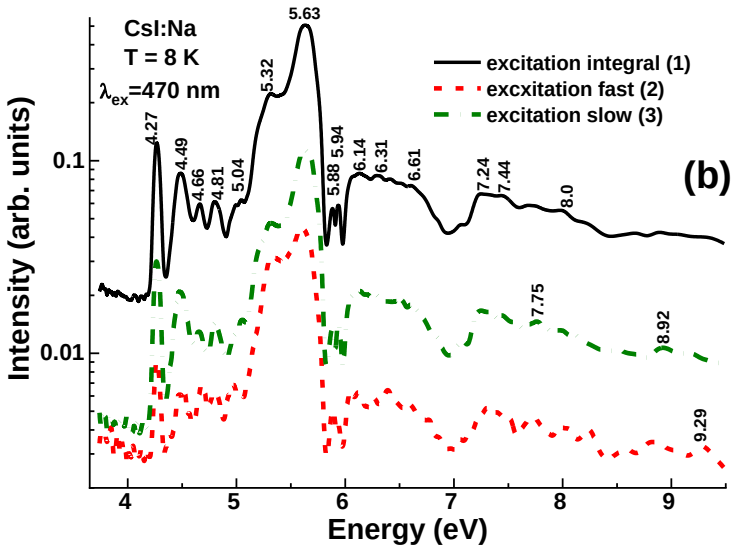

Fig.5. PLE spectra in the logarithmic scale of defect-related centres emitted in the band at 476 nm (b), registered at 470 nm in the CsI:Na crystal at 8 K.

comparison with the PLE spectra of Na_{Cs} center luminescence (Fig. 4), the defect-related spectrum exhibits a strong band in the exciton range, with peaks at 5.32 and 5.53 eV, corresponding to the formation of excitons bound to these centers. In addition to these bands, other PLE bands appear at 4.27, 4.49, 4.66, 4.81, and 5.04 eV (Table 1), which are most likely related to intrinsic transitions of these centers. A definitive determination of their nature based on the spectral positions of these bands and the decay kinetics (Fig. 6) requires a more detailed investigation, including EPR analysis (Fig. 5).

5. PL Decay Kinetics of Different Centers in CsI:Na Crystal

5.1 PL Decay Kinetics of STE Centers

The PL decay kinetics of STE in both on-center and off-center configurations, measured at 290 nm and 340 nm in the vicinity of the σ- and π- bands in CsI:Na crystal at 8 K under excitation by SR at characteristic points of the PLE spectra (Fig. 2, Table 1), are shown in Fig. 6a and Fig. 6b, respectively.

Due to the non-exponential nature of the decay kinetics, all decay curves of the respective centers were approximated using two- or three-component exponential functions: $I = \Sigma A_i \exp(-t/\tau_i) + A_S$, where i = 2 or 3, and A_S (the so-called "slow pedestal") is proportional to the content of slow components. These components could not be accurately determined within the short (1.2–193 ns) time interval for decay time measurements. The respective decay times τ_i (i = 3) are presented in Table 2.

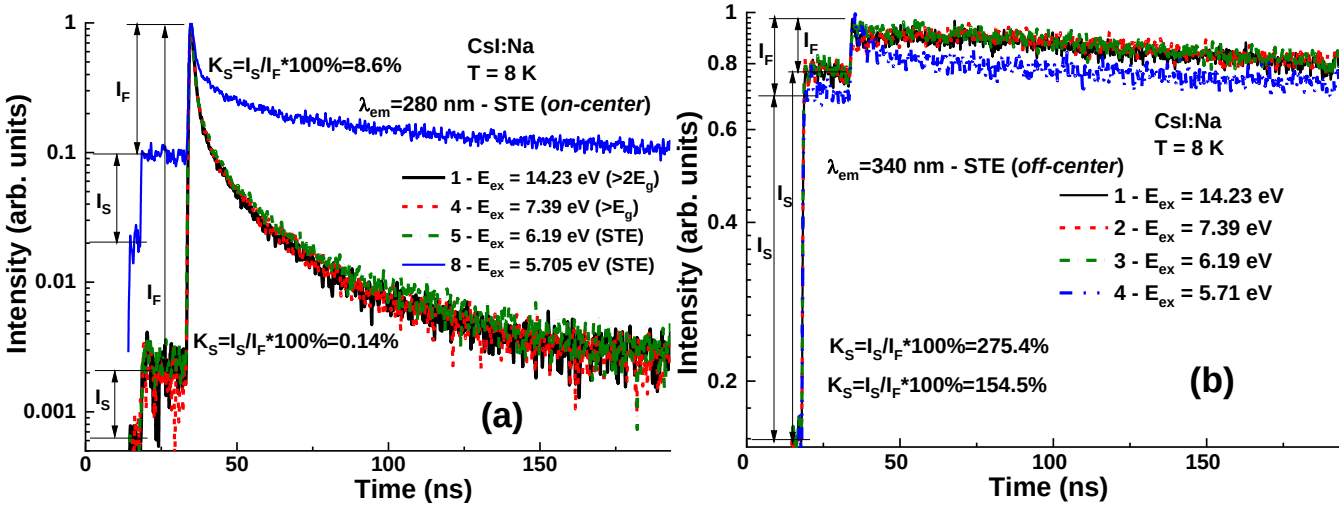

Fig. 6. Decay kinetic of luminescence *on-center* STE (a) and *on-center* STE (a) registered in σ (a) and π (b) bands peaked at 280 nm (a) and 340 nm (b), respectively, in CsI:Na crystal at 8 K.

Table 2. Parameters of approximation of the decay curves of the different emission centers in CsI:Na crystals, presented in Figs. 6 and 7. n. m. – not measured

Type of center	Ex. energy, eV	t_1, ns	t_2, ns	t_3, ns	K_S, %
STE (*on-center*)	14.23	2.6	14.3	64.4	0.11
	7.39	2.55	15.3	62.3	0.12
	6.19	2.62	16.35	62.2	0.14
	5.705	3.8	77.3	148.4	8.6

STE (*off-center*)	14.23	0.9	540	890	n. m.
	7.39	rise time; n. m.	-275 (rise time)	1220	n.m.
	6.19	rise time; n. m.	- 66.7 (rise time)	513	275.4
	5.71	1.3	364	1060	154.5
BSE (Na_{Cs})	14.23	1.4	9.8	1320	8.6
	7.38	2.7	28.5	1310	12.4
	5.63	16.2	56.1	1770	17.0
	5.33	12.5	47.0	1295	22.5
BSE (defect-related center)	5.63	18.7	105	2560	69.9

Under excitation by SR with energies above the band gap of the CsI host (14.23 eV and 7.39 eV), as well as at 6.19 eV, corresponding to the singlet excited state of the *on-center* STE, the decay kinetics are very fast (Fig. 6a), and the corresponding $\boldsymbol{\tau_i}$ values vary from several nanoseconds to several tens of nanoseconds (Table 2). However, under SR excitation with an energy of 5.705 eV, related to the triplet excited state of the *on-center* STE, the decay kinetics are much slower, and the respective $\boldsymbol{\tau_i}$ values range from several nanoseconds to a few hundred nanoseconds (Table 2). We also calculated the content of slow components K_s using the formula: $Ks=I_S/I_F*100\%$, under SR excitation with energies above $2E_g$ (14.23 eV) and E_g (7.38 eV), as well as at the singlet and triplet excited states of the on-center STE (6.19 eV and 5.705 eV, respectively). The calculated values were 0.11%, 0.12%, 0.14%, and 8.6%, respectively (Fig. 6a).

Conversely, under excitation by SR with energies above the CsI band gap (14.23 eV and 7.39 eV), and at 6.19 eV, corresponding to the triplet excited state of the off-center STE, the decay kinetics become very slow (Fig. 6b). For this reason, we could only correctly estimate the corresponding values of τ_3, which shift into the microsecond range (Table 2). However, under SR excitation at 5.71 eV, related to the singlet excited state of the off-center STE, the decay kinetics are slightly faster, and the respective $\boldsymbol{\tau_i}$ values range from several nanoseconds to several hundred nanoseconds (Table 2).The calculated content of slow components K_s under excitation at the triplet and singlet excited states of the off-center STE (6.19 eV and 5.71 eV, respectively) yielded significantly high values of 275.4% and 154.5%, respectively (Fig. 6b).

However, it is important to note that due to the substantial overlap of the PLE spectra for the singlet and triplet states of both on-center and off-center STE configurations, accurately separating the respective decay profiles and estimating precise luminescence decay times within such short time intervals remains challenging. Nevertheless, assessing general trends in the luminescence properties of different STE configurations in CsI crystals and understanding their energy structure through luminescence studies under SR excitation remains undoubtedly valuable.

5.2 PL Decay Kinetics of Na_{Cs} Centers

The PL decay kinetics of the Na_{Cs} center and defect-related center (DC), measured at 415 nm and 470 nm, respectively, in a CsI:Na crystal at 8 K under excitation by SR at characteristic points of the PLE spectra (Fig. 2, Table 1), are shown in Fig. 7a and Fig. 7b.

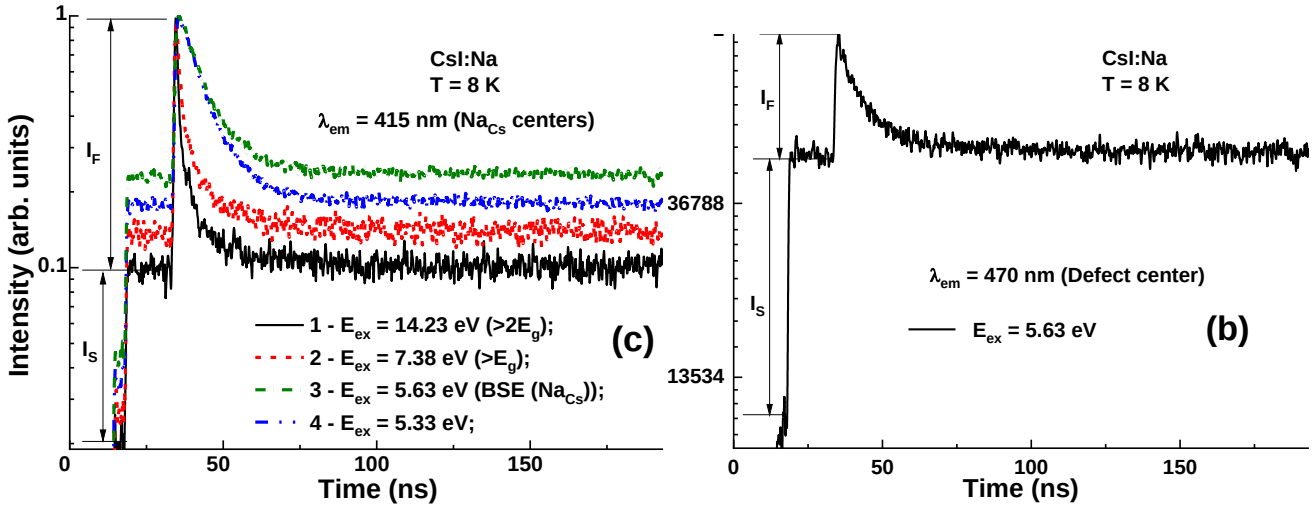

Fig.7. Decay kinetic of luminescence Na_{Cs} centers, registered at 420 nm (a), and defect-related centers, registered at 470 nm (b) in CsI:Na crystals at 8 K.

In general, the decay kinetics of the Na_{Cs} center are typical for the decay profiles of excitons bound to isoelectronic impurities, such as Sc^{3+} and Ga^{3+} ions in Al_2O_3 sapphire [16, 17], and Sc^{3+} and La^{3+} ions in YAG and LuAG garnets [21, 22] as well as YAP perovskite [23]. The decay curve of such centers usually possesses a very fast initial component in the nanosecond range, followed by an intensive slow component, most likely corresponding to radiative transitions from the singlet and triplet excited states of BSE (Na_{Cs}) and excitons bound to defect-related centers.

Due to the non-exponential nature of the decay kinetics of these centers, their PL decay profiles were approximated using a three-exponential function $I = \Sigma A_i \exp(-t/\tau_i) + A_S$ (A_S - amplitude of slow pedestal), where A_S represents the amplitude of the slow pedestal. The respective decay times τ_i (i = 3) are presented in Table 2.

The slow component fraction K_S was calculated using the formula: $Ks = I_S/I_F*100\%$, under excitation with energies above $2E_g$ (14.23 eV) and E_g (7.38 eV) values, as well as the triplet and singlet excited states of BSE (Na_{Cs}) (5.63 and 5.33 eV) and BSE (DC) (5.63 eV). The calculated values were 8.64% and 12.4%, and 17.0% and 22.5%, respectively (Fig. 7a).

6. Discussion

The radioluminescence (RL) of CsI:Na crystals can be stimulated by excitation from both X and γ-rays, as well as optical excitation with energies surpassing the CsI band gap, approximately 6.6 eV (referencing Figs. 2 and 3 and literature [8]). This excitation creates a core hole, which can evolve into a self-trapped hole, represented as a diiodine I_2^- molecule (V_K centers), or a self-trapped hole surrounding the Na impurity located in the second coordination sphere (V_{KA} centers).

In this context, the Na_{Cs} isoelectronic dopant serves a dual function. Initially, it can localize an electron from the conduction band, subsequently binding with a hole from the valence band to form

excitons bound to the Na impurity. This process results in radiative relaxation, producing emissions in the band peaked at 417 nm (2.96 eV) (see Fig. 1).

Despite the relatively high concentration of Na (0.3 at.%) in CsI:Na crystals, the formation of self-trapped excitons (STE) ($e + V_K$) and localized excitons around the dopant (LE) ($e + V_{KA}$) remains plausible. These excitons exhibit characteristic radiative relaxations in the ultraviolet range, with emission bands peaking at 290 nm (4.26 eV), 342 nm (3.62 eV), as well as at 313 nm (3.955 eV), and 360 nm (3.44 eV). The two emission bands associated with STE and LE centers correspond to σ- and π-components, which relate to fast singlet-singlet and slower triplet-singlet transitions of these centers, respectively.

Several recombination mechanisms are viable in CsI:Na crystals, each associated with luminescence from Na_{Cs}, V_K, and V_{KA} centers:

1. *Long-Distance Tunneling Recombination*: This mechanism is akin to donor-acceptor pair interactions in semiconductors. The processes can be represented as:
   - $[Na_{Cs} + e] + V_K (I_2^-) \rightarrow [Na_{Cs}] + h\nu$;
   - $[Na_{Cs} + e] + V_{KA} (I_2^-) \rightarrow [Na_{Cs}] + h\nu$;
2. *Long-Distance Electron Transfer:* This process forms STE or LE intermediates:
   - $[Na_{Cs} + e] + V_K \rightarrow [Na_{Cs}] + [V_K + e] \rightarrow [Na_{Cs}] + h\nu$;
   - $[Na_{Cs} + e] + V_{KA} \rightarrow [Na_{Cs}] + [V_{KA} + e] \rightarrow [Na_{Cs}] + h\nu$;
3. *Capture to Form Sodium-Localized Excitons*: This mechanism describes the formation of localized excitons:
   - $[Na_{Cs}\text{-}V_{KA}] + e \rightarrow [Na_{Cs} + V_{KA} + e] \rightarrow [Na_{Cs}] + h\nu$;
4. *Recombinative Capture of a Free Electron:* This leads to the formation of bound state excitons:
   - $[Na_{Cs} + V_K] + e \rightarrow [Na_{Cs}] + h\nu$.

While these four mechanisms encompass the primary pathways for recombination in CsI:Na crystals, it is important to acknowledge that there are numerous other potential mechanisms with varying levels of complexity. However, the mechanisms outlined above incorporate the most significant interactions involved in the luminescence processes of these crystals.

In summary, the interplay between exciton formation and various radiative recombination mechanisms in CsI:Na crystals under excitation with different energies provides a rich framework for understanding radioluminescence properties of this scintillator. Future studies should aim to further elucidate these mechanisms, particularly through time-resolved spectroscopic techniques and EPR measurements that can provide insights into the dynamics of exciton behaviour and the influence of varying dopant concentrations on luminescent properties.

Conclusions

The study outlined investigates the luminescence properties and energetic structure of luminescence centers in CsI:Na (0.3 at.%) crystal, focusing on the peculiarities of the emission self-trapped excitons

(STE), as well as excitons *localized* around (LE) and bound (BSE) with sodium isoelectronic impurity (Na_{Cs}) and defect-related centers. Using synchrotron radiation (SR) excitation across a wide 3.7-25 eV energy range, namely in the exciton range (5-6 eV), in the onset of interband transitions (6.3-6.7 eV) and in the range of multiplication of electronic excitation in the CsI host (7-22 eV), the research identifies several significant findings regarding structure of the emission spectra and excitation spectra as well as decay kinetic of mentioned centers.

The emission spectra of CsI:Na (0.3 at.%) crystal reveal a complex superposition of different luminescence types, including: (i) *STE luminescence* with distinct emission peaks at 282 nm and 340 nm attributed to *on-center* and *off-center* configurations of STE; (ii) *LE luminescence* in weaker emission bands peeked at 313 nm and 364 nm corresponding to t*on-center* and *off-center* configurations LEs around Na_{Cs} centers; (iii) *Sodium Impurity Emission* in a dominant band peaked at 417 nm related to excitons bound with Na_{Cs} center; (iv) *Vacancy-Localized Excitons* luminescence in a low-intensity band peaked at 470 nm corresponding to excitons localized at vacancy aggregates, and (v) *Defect-Related Emissions*: in weak bands peaking at 570 nm and 690 nm likely corresponding to excitons localized at non-vacancy defects.

The study also quantifies the energy of STE creation, finding values of 5.72 eV and 6.16 eV for σ-configuration components, and 5.88 eV and 6.15 eV for π-configuration components. Additionally, energies associated with the creation of bound excitons with Na_{Cs}, been equal to 5.42 to 5.695 eV, and aggregate defects centers, been equal to 5.32 and 5.63 eV were determined for the slow and fast components, respectively, providing insights into their energetic characteristics.

Analysis of STE luminescence decay kinetic processes reveals strong differences depending on excitation energy. Excitation by SR with energies above the band gap and those related to the singlet state of STE result in fast decay kinetics, with lifetimes ranging from several nanoseconds to tens of nanoseconds. In contrast, excitation related to the triplet state yields slower decay kinetics, with lifetimes extending from several nanoseconds to a few hundred nanoseconds. The decay profiles for Na_{Cs} and defect-related centers exhibit characteristics typical of excitons bound to isoelectronic impurities, showcasing a fast initial decay followed by slower tools related to the transitions from singlet and triplet excited states, respectively.

This comprehensive analysis enhances the understanding of luminescence mechanisms in CsI:Na crystals and the role of various excitonic states and isoelectronic impurities in these processes. The findings could have implications for applications CsI:Na crystal as scintillators in optoelectronics devices, where tailored luminescent properties are strongly required.

Funding: The research work has been funded by Science Committee of the Ministry of Science and Higher Education of the Republic of Kazakhstan (Grant No. AP26100001) and Polish National Centre of Science (NCN) in frame of Opus 24 LAP No 2022/47/I/ST8/02600 project.

References

1. https://www.epic-scintillator.com/CsI(Na)-crystal.

2. https://www.shalomeo.com/Scintillators/Scintillation-Crystal-Materials/CsI-Na%20/product-392.html

3. http://www.amcrys.com/details.html?cat_id=146&id=4280

4. O.L. Hsu and C.W. Bate. Absorption and emission due to localized excitons in CsI:Na. Journal of Luminescence 15 (1977) 77.

5. C K Ong, K S Song, R Monnier and A M Stoneham. Electronic structure and luminescence of CsI:Na. 1979) J. Phys. C. Solid state, 12 (1979) 4641- 4646.

6. Jin-Cherng Hsu, and Yu-Shen Ma. Luminescence of CsI and CsI:Na Films under LED and X-ray Excitation. Coatings 9 (2019) 751.

7. A.H. Kayal, Y. Mori, C. Jaccard and J. Rossel, Luminescence processes in CsI doped with Na^+ and K+ ions. Solid State Communications, 35 (1980) 457—460.

8. Taketoshi Kawai, Satoru Nagata, and Takeshi Hirai. Comparison of Luminescence Properties of CsI Crystals Activated with Ag, Au, and Tl Ions at Room Temperature. Japanese Journal of Applied Physics 52 (2013) 082401.

9. A. Belsky, A. Vasil'ev, V. V. Mikhailin, A.V. Gektin, P. Martin, C. Pedrini, D. Bouttet. Experimental study of the excitation threshold of fast intrinsic luminescence of CsI. Physical Review B 49 (1994) 13197.

10. M. Kirm, L. Jonson, F. Savikhin, G. Svensson, S. Vielhauer and G. Zimmerer. Relaxation of electronic excitation in CsI crystals studied by synchrotron radiation and pulsed electrons. Radiation Measurements 29 (1998), 257-261.

11. S. V. Myagkota, A. S. Pushak, G. B. Stryganyuk, T. M. Demkiv, and L. S. Demkiv. Spectral-kinetic luminescent characteristics of CsI-Ba single crystals. Phys. Status Solidi B 247 (2010) 393–397.

12. V. B. Mikhailik, V. Kapustyanyk, V. Tsybulskyi, V. Rudyk, and H. Kraus. Luminescence and scintillation properties of CsI: A potential cryogenic scintillator. Phys. Status Solidi B 252 (2015) 804–810.

13. Yu. Zorenko, T. Voznyak, R. Turchak, A. Fedorov, K. Wiesniewski, M. Grinberg. Luminescent and scintillation properties of CsI:Tl films grown by the liquid phase epitaxy method. Phys. Status Solidi A. 2010. V. 207, No. 10. P. 2344–2350.

14. J.A. Valbis. Luminescence of bound excitons in alkali-halide crystals with first-group cation impurities. Opt. Spectros (USSR) (Engl. Transl.), 21, 1966, 106-9.

15. Y. Zorenko. Luminescence of isoelectronic impurities and anti-site defects in garnets. Phys. Stat. Sol. (c). 2 (2005) 375-379.

16. J.L. Janson, P.A. Kulis, Z.A. Rachko, J. Springis, I.A. Tale, and J.A. Valbis. Luminescence of Ga-Doped Al_2O_3 Crystals. Phys. Stat. Sol. (b) 120 (1983) 511.

17. M. Kirm and G. Zimmerer. Self-trapping and multiplication of electronic excitations in Al_2O_3 and Al_2O_3:Sc crystals. Phys. Rev. 60 (1999) 502-510.

18. Maria da Conceição Costa Pereira, Tufic Madi Filho, José Roberto Berretta, Lucas Faustino Tomaz, Miriam Nieri Madi. Optical properties and radiation response of Li ion-doped CsI scintillator crystal RAP Conference Proceedings, 4 (2019) 131–135.

19. Maria C. C. Pereira, Tufic M. Filho, Margarida M. Hamada. Development of crystals based on cesium iodide for measurements of gamma radiation and alpha particles. Nukleonika, 54 (2009) 151−155.

20. K. Shunkeyev 1, A. Kenzhebayeva 1, A. Krasnikov, V. Nagirnyi, Sh. Sagimbayeva, D. Sergeyev 1, A. Tilep, Zh. Ubaev, A. Lushchik. Luminescence of bound excitons in the field of local lattice deformation caused by sodium impurity ions in KCl:Na single crystals. Optical Materials: X, 25 (2025) 100395.

21. Yu. Zorenko, V. Gorbenko, A. Voloshinovskii, G. Stryganyuk, S. Nedilko, V. Degoda, O. Chykova. Luminescence of Sc-related centers in single crystalline films of $Lu_3Al_5O_{12}$ garnet. Phys. stat. sol. (c). 2 (2005) 105-108.

22. Yu. V. Zorenko. Luminescence of La^{3+} and Sc^{3+} Isoelectronic Impurities in $Lu_3Al_5O_{12}$ Single Crystalline Films. Optics and Spectroscopy, 100 (2006) 572-580.

23. Yu. Zorenko, V. Gorbenko, T. Voznyak, T. Zorenko, M. Nikl, K. Nejezchleb. Luminescence of La^{3+} and Sc^{3+} impurity centers in $YAlO_3$ single-crystalline films. Journal of Luminescence, 128 (2008) 595-602.

24. Yu. Zorenko, A. Voloshinovskii, V. Savchyn, T. Vozniak, M. Nikl, K. Nejezchleb, V. Mikhailin, V. Kolobanov, D. Spassky. Exciton and antisite defect–related luminescence in $Lu_3Al_5O_{12}$ and $Y_3Al_5O_{12}$ garnets. Phys. Stat. Sol. (b). 2007. V.244, No 6. P.2180-2189.

25. Yu. Zorenko, A. Voloshynovskii, V. Vistovsky, M. Grinberg, A. Kornylo, T. Łukasiewicz, M. Świrkowicz. The anti-site defect-related luminescence in $(LaLu)_3Lu_2Ga_3O_{12}$ garnet single crystals Phys. Stat. Sol. (b). 244 (2007) 3271-3278.

26. T. Zorenko, V. Gorbenko, A. Petrosyan, W. Gieszczyk, P. Bilski, Yu. Zorenko. Intrinsic and defect-related luminescence of $YAlO_3$ and $LuAlO_3$ single crystals and films, Optical Materials, 86 (2018) 376–381.

27. V. Kolobanov, V. Mikhailin, N. Petrovnin, D. Spassky, Yu. Zorenko. Exciton creation in $LuAlO_3$ single crystalline film. Phys. Stat. Sol. (b). 2006. V.243. P.R60–R62.

28. Yu. Zorenko, T. Zorenko, T. Voznyak, O. Sidletskiy. Intrinsic luminescence of Lu_2SiO_5 (LSO) and Y_2SiO_5 (YSO) orthosilicates, Journal of Luminescence, 137 (2013) 204–207.

29. Yu. Zorenko, T. Voznyak, V.V. Gorbenko, A. Doroshenko, A. Tolmachev, R. Yavetskiy, I. Petrusha, V. Turkevich, Comparative study of the luminescence of $Y_3Al_5O_{12}$ nanoceramics and single crystals under excitation by synchrotron radiation, Optical Materials, 35 (2013) 2049–2052.

30. T. Zorenko, V. Gorbenko, N. Dulina, N. Matveevskaya, R. Yavetskiy, N. Babayevskaya, Yu. Zorenko. Comparative study of the luminescent properties of oxide compounds under synchrotron radiation excitation: Lu_2O_3:Eu nanopowders, ceramics and films, Journal of Luminescence, 199 (2018) 461-464.